Journal of Neuropathology and Experimental Neurology

Vol. 62, No. 12
December, 2003
pp. 1287–1301

Vascular Pathology in Alzheimer Disease: Correlation of Cerebral Amyloid Angiopathy and Arteriosclerosis/Lipohyalinosis with Cognitive Decline

DIETMAR RUDOLF THAL, MD, ESTIFANOS GHEBREMEDHIN, MD, MARIO ORANTES, MD, AND OTMAR D. WIESTLER, MD

Abstract. Sporadic, late-onset Alzheimer disease (AD) constitutes the most frequent cause of dementia in the elderly population. AD-related pathology is often accompanied by vascular changes. The predominant vascular lesions in AD are cerebral amyloid angiopathy (CAA) and arteriosclerosis/lipohyalinosis (AS/LH). The present study was carried out to examine the coincidence of these small vessel pathologies during the development of cognitive deficits, amyloid β-protein (Aβ) deposition, and neurofibrillary tangle (NFT) formation in sporadic late-onset AD. We correlated the clinical dementia rating (CDR) score, the sequential extension of AD-related Aβ deposition into different parts of the brain, and the extension of NFTs to involve more brain regions with the distribution of CAA and AS/LH in 52 human autopsy brains. The extension of CAA and AS/LH to involve different areas of the brain was associated with a rise of CDR scores and an increase in the extension of Aβ deposition and NFT generation. AD cases showed a higher number of regions with CAA and AS/LH compared to nondemented patients with AD-related pathology and controls. Moreover, we demonstrated a hierarchical sequence in which the different regions of the brain exhibited CAA and AS/LH-affected vessels, allowing the distinction of 3 stages in the development of CAA and AS/LH. The first stage of CAA involved leptomeningeal and neocortical vessels. The second stage was characterized by additional Aβ deposition in allocortical and midbrain vessels. Finally, in a third stage, CAA was observed in the basal ganglia, the thalamus, and in the lower brainstem. In contrast, AS/LH initially affected the basal ganglia in stage A. In stage B this pathology made inroads into the deep white matter, the leptomeningeal arteries of the cortex, the cerebellum, and into the thalamus. Stage C was characterized by AS/LH in brainstem vessels. Our results demonstrate widespread CAA and AS/LH to be associated with the development of cognitive deficits in AD. A combination of both CAA and AS/LH may, therefore, contribute to neurodegeneration in AD. These data also suggest that small vessel disease due to arteriosclerosis and fibrolipohyalinosis is a potential target for the treatment of AD.

Key Words: Alzheimer disease; Amyloid β-protein; Apolipoprotein E; Arteriosclerosis/Lipohyalinosis; Cerebral amyloid angiopathy; Dementia.

INTRODUCTION

Sporadic late-onset Alzheimer disease (AD) is the most frequent cause of dementia in the elderly population. The extracellular deposition of amyloid β-protein (Aβ) and the intracellular generation of neurofibrillary tangles (NFTs) represent histopathological hallmarks of AD (1–4). Cerebrovascular changes often accompany AD-related pathology (5–10). The most common cerebrovascular diseases of small blood vessels in the aged brain include cerebral amyloid angiopathy (CAA) and arteriosclerosis/lipohyalinosis (AS/LH) (5, 7, 10–12). CAA prevails in leptomeningeal and neocortical vessels and less frequently in the cerebellar cortex (9, 13–15). On the other hand, AS/LH predominantly occurs in vessels of the striatum, the deep white matter, and of the leptomeninges (10, 11, 16).

In the aged brain with AD-related pathology, the extension of NFTs (the term extension in the context of this article is defined as the extension of a given pathology to involve more brain regions) and that of Aβ deposits correlate with the degree of dementia (17–21) and show a hierarchical pattern in the involvement of different brain regions (2, 17, 19, 22). Although it is well known that AD patients show more severe and widespread CAA compared to nondemented patients (13, 15, 23), the detailed anatomical distribution of CAA and other microvascular changes in relation to the development of cognitive deficits, NFTs, and Aβ deposits has not been systematically analyzed in the development of AD. It also remains to be studied whether the formation of vascular changes in the AD brain follows a similar anatomical sequence as Aβ deposition (17, 22) or NFT formation (2, 19).

To identify a role of CAA and AS/LH in AD, we assessed the development of CAA and AS/LH throughout 19 different brain regions in 52 human autopsy brains, including AD cases, nondemented cases with AD-related pathology, and controls without AD-related pathology. Our findings indicate a distinct sequence of CAA and AS/LH involving different brain regions. Both lesions are associated with the development of dementia in late-onset AD.

From Department of Neuropathology (DRT, ODW), University of Bonn Medical Center, Bonn, Germany; Department of Clinical Neuroanatomy (EG), Johann Wolfgang Goethe University, Frankfurt am Main, Germany; Department of Pathology (MO), Municipal Hospital Offenbach am Main, Offenbach am Main, Germany.

Correspondence to: Dietmar R. Thal, MD, Department of Neuropathology, University of Bonn Medical Center, Sigmund Freud Strasse 25, D-53105 Bonn, Germany. E-mail: Dietmar.Thal@uni-bonn.de

Supported by DFG-grants No. TH 624/4–1 (DRT) and GH 12/1–2 (EG) and BONFOR-grants No. O-154.0041 (DRT) and O-154.0043 (DRT).

MATERIALS AND METHODS

Clinical Assessment

Fifty-two human autopsy brains of both genders, aged 61 to 97 years, including 17 AD cases, 26 nondemented individuals with AD-related pathology (ADRP) cases, 4 cases without any AD-related pathology (controls), and 5 cases with AD-related pathology and clinical records providing no information about the cognitive status, were investigated (Table 1). To study all stages in the development of AD, we selected cases from a larger unselected autopsy series using the following criteria: 1) 60 years of age or older, 2) a minimum of 4 cases in each phase of AD-related Aβ pathology (Aβ phases) (17) and controls without AD-related pathology, and 3) inclusion of AD and nondemented cases. The presence or absence of CAA or AS/LH was not used as selection criteria. Familial AD, Down syndrome, Creutzfeldt-Jacob disease, familial CAA, and inflammatory diseases of the brain or the vessels were not included. Also excluded were cases with a history of previous head trauma, large brain tumors, or with vascular malformations. Our goal was to minimize factors that could interfere with vascular Aβ deposition and arteriosclerotic vascular changes, thereby enabling us to study more accurately the effects of degenerative microvascular lesions on the development of sporadic late-onset AD-related Aβ deposits, NFTs, cognitive deficits, as well as on the development of AD in general. Cases with argyrophilic grain disease and AD-related pathology were included in this study (Table 1).

All patients had been examined 1 to 4 weeks prior to death by different clinicians according to standardized protocols. The protocols included the assessment of cognitive function and recorded the ability to care for and dress self, eating habits, bladder and bowel continence, speech patterns, writing and reading, short-term and long-term memory, and orientation within the hospital setting. These data were used to retrospectively assess the clinical dementia rating (CDR) scores for each patient (24) (Table 1). For this purpose, the information from the clinical files was transformed into CDR levels according to the standard CDR-protocol (24). AD was diagnosed according to recently published consensus criteria (25). Cases with AD-related NFT and/ or Aβ pathology that were clinically diagnosed as cognitively normal (CDR = 0) were categorized as putative ADRP cases. These cases also include Aβ-only and NFT-only cases. The controls showed no dementia (CDR = 0). For cases 48 to 52, clinical recordings did not allow assessment of CDR scores (Table 1).

Neuropathological Analysis

Tissue was fixed in a 4% aqueous solution of formaldehyde. We excised blocks from the anterior, middle, and posterior medial temporal lobes and embedded them in polyethylene glycol and in paraffin. The polyethylene glycol blocks were microtomed at 100 μm and paraffin material at 10 μm. We applied this procedure to paraffin sections of the superior frontal gyrus, the superior parietal lobe, Brodmann areas 17, 18 and 19, cingulate gyrus, basal ganglia, basal nucleus of Meynert, septum, hypothalamus, thalamus, midbrain, pons, medulla oblongata, and the cerebellum. Gallyas silver-staining was used to detect AD-related neurofibrillary pathology and the Campbell-Switzer silver method to assess the presence of amyloid plaques (26). For topographical orientation and neuropathological diagnosis, we stained paraffin and polyethylene glycol sections with aldehyde fuchsin-Darrow red for lipofuscin pigment and Nissl material or hematoxylin and eosin (H&E). The Prussian blue method was used to detect hemosiderin in macrophages; positive and negative controls were carried out. The Elastica van Gieson staining method was used to identify vascular changes. To verify the degree of AD-related pathology, staging of NFTs according to published criteria (2, 25) (Table 1) was performed. Phases of β-amyloidosis (Aβ phase) were determined as described recently (17). The Aβ phases represent the amyloid burden of the brain corresponding to the number of brain regions exhibiting Aβ deposits (17, 22): 0 = no Aβ, 1 = neocortical Aβ, 2 = neo- and allocortical Aβ, 3 = cortical, diencephalic and striatal Aβ, 4 = cortical, diencephalic, striatal and midbrain Aβ, 5 = cortical, diencephalic, striatal, midbrain, pontine, and cerebellar Aβ.

Assessment of cerebral infarction and intracerebral hemorrhage was performed macroscopically for gross lesions and microscopically for the regions listed by studying H&E-stained sections or aldehyde fuchsin-Darrow red-stained sections. To compare the extension of small vessel changes in cases with and without cerebral infarction, the presence of cerebral infarcts was noted regardless of their age, size, and etiology in a dichotomized manner. It was not differentiated between cases with multiple and single infarcts. To compare the extension of small vessel changes in cases with and without intracerebral hemorrhage, the presence of intracerebral hemorrhage was noted regardless of the age, size, and etiology of the hemorrhage in a dichotomized manner. It was not differentiated between multiple and single hemorrhages. Those cases with intracerebral hemorrhage were further subclassified into cases with clinically relevant hemorrhages and into cases with clinically silent hemorrhages in a dichotomized manner. The diagnosis of clinically relevant intracerebral hemorrhages was restricted to cases with intracerebral hemorrhage as the morphological correlate for neurological deficits. Clinically silent hemorrhages usually represented small hemorrhages in patients without any neurological symptoms.

The presence of atherosclerosis was examined macroscopically in the basal arteries (circle of Willis) and noted in a dichotomized manner. Immunohistochemistry was performed on 10-μm paraffin sections from the superior frontal gyrus, superior parietal lobe, Brodmann areas 17, 18 and 19, cingulate gyrus, anterior medial temporal lobe including the entorhinal region, the middle and posterior medial temporal lobe with the hippocampus, basal ganglia, basal nucleus of Meynert, septum, hypothalamus, thalamus, midbrain, pons, medulla oblongata, and the cerebellum. Sections were immunostained after formic acid pretreatment with the following antibodies directed against Aβ: $A\beta_{17-24}$ (Signet, Dedham, MA: 4G8, 1/5000, 72 h at 4°C), and $A\beta_{1-17}$ (Signet: 6E10, 1/2000, 24 h at 22°C). The primary antibodies were detected with a biotinylated secondary antibody and the ABC complex (Vectastain: Vector Laboratories, Burlingame, CA), then visualized with 3,3 diaminobenzidine-HCl. Blank controls as well as positive and negative controls were carried out. Paraffin sections were counterstained with hematoxylin.

TABLE 1
List of Cases

Case.	Age	Gender	Diagnosis	Aβ Phase	NFT stage	CDR	CAA stage	AS/LH stage	APOE
1	66	f	—	0	0	0	0	0	3/3
2	62	m	—	0	0	0	0	0	3/3
3	63	m	—	0	0	0	0	B	3/3
4	69	f	—	0	0	0	0	0	2/3
5	61	f	ADRP	0	1	0	0	B	3/4
6	77	m	ADRP	0	2	0	0	B	3/3
7	61	f	ADRP	1	0	0	0	A	3/4
8	67	m	ADRP	1	1	0	1	A	3/3
9	75	f	ADRP	1	1	0	1	A	2/3
10	75	m	ADRP	1	2	0	0	A	3/3
11	71	f	ADRP	1	2	0	1	C	3/4
12	82	f	ADRP	1	3	0	0	C	3/4
13	65	f	ADRP	2	0	2	1	B	3/4
14	64	m	ADRP	2	1	0	0	B	3/3
15	65	m	ADRP	2	1	0	0	0	3/4
16	71	m	ADRP	2	1	0	1	B	3/3
17	69	m	ADRP	2	1	0	1	A	3/3
18	74	f	ADRP	2	1	0	0	B	3/3
19	97	m	ADRP	2	2	0	0	C	3/3
20	72	m	ADRP	2	3	0	0	B	3/3
21	71	m	ADRP	3	1	0	0	A	3/3
22	67	f	ADRP	3	1	0	2	B	3/3
23	85	m	ADRP	3	1	0	1	C	3/3
24	67	m	ADRP	3	2	0	2	A	2/3
25	83	f	ADRP	3	3	0	1	A	2/3
26	84	f	ADRP	3	3	0	1	B	3/3
27	63	f	ADRP	4	3	0	0	B	3/3
28	85	f	ADRP	4	3	0	0	C	3/3
29	87	m	ADRP	4	3	0	3	C	3/4
30	83	f	ADRP,AG	4	4	0	2	C	2/2
31	82	m	AD,AG	3	2	2	0	B	3/4
32	79	m	AD	4	2	2	2	C	3/4
33	81	f	AD,AG	4	2	1	0	C	3/4
34	78	m	AD	4	4	1	1	B	3/3
35	81	f	AD	4	4	3	1	C	3/3
36	85	m	AD	5	3	2	3	C	3/4
37	80	m	AD	5	3	2	2	C	3/4
38	66	f	AD	5	4	3	3	B	n.d.
39	89	f	AD	5	4	2	2	B	3/4
40	83	m	AD	5	4	3	2	B	3/3
41	88	f	AD	5	4	3	2	C	3/3
42	97	f	MCI-AD	5	4	0.5	2	C	3/4
43	89	f	AD	5	5	3	2	C	3/4
44	83	m	AD	5	5	3	3	B	4/4
45	79	f	AD	5	5	3	3	B	3/4
46	68	f	AD	5	6	1	1	B	3/3
47	86	f	AD	5	6	3	2	B	3/3
48	82	m	AG	1	1	n.d.	1	B	3/4
49	66	m	n.d.	2	2	n.d.	1	A	3/4
50	90	f	n.d.	5	3	n.d.	3	B	3/3
51	88	m	n.d.	5	4	n.d.	3	B	4/4
52	74	m	n.d.	5	4	n.d.	2	C	n.d.

Case number, age in years, gender, neuropathological diagnosis, Aβ phase, NFT stage, CDR score, CAA, AS/LH stage, and APOE genotype of the cases investigated in this study. Abbreviations: m = male, f = female, AG = few argyrophilic grains, AD = Alzheimer's disease (25), ADRP = nondemented cases with AD-related pathology, MCI-AD = Mild cognitive impairment and AD-related pathological changes, n.d. = diagnosis and CDR score were not determined because of insufficient clinical recordings.

Apolipoprotein E Genotyping

For genotyping of apolipoprotein E (APOE), genomic DNA was extracted either from unfixed frozen brain tissue or from the paraffin-embedded cerebellar cortex. For suitable DNA templates, a one-step polymerase chain reaction (PCR) was used, followed by standard restriction isotyping with the restriction enzyme *Hha*I (27). For DNA templates from formaldehyde-fixed specimens, a semi-nested PCR assay was employed (28). This method facilitates reliable APOE genotyping of DNA from archival tissue specimens by enhancing the yield of the PCR product. Positive and negative controls were carried out.

Morphological Analysis

Morphological analysis of CAA was based on anti-$A\beta_{17-24}$ immunostained sections. It has been shown that the anti-$A\beta_{17-24}$ antibody sufficiently detects all CAA-affected cerebral blood vessels (29–31). For the superior frontal gyrus, superior parietal lobe, Brodmann areas 17, 18 and 19, cingulate gyrus, anterior MTL including the entorhinal region, middle and posterior MTL with the hippocampus, basal ganglia, basal nucleus of Meynert, septum, hypothalamus, thalamus, midbrain, pons, medulla oblongata, and the cerebellum, we noted the types of vessels involved in CAA, identified their locations (leptomeninges, cerebral cortex, and white matter), and recorded the number of the above mentioned regions with vessels exhibiting CAA in order to determine the extension of CAA.

Extension of CAA = Number of brain regions exhibiting CAA-affected vessels

Aldehyde fuchsin-Darrow red-, H&E-, and Elastica van Gieson-stained sections were used for the detection of AS/LH changes in vessels. Perivascular lipid-containing macrophages around lipohyalinotic vessels were distinguished from hemorrhage-derived siderophages in Prussian blue-stained sections. The diagnosis of AS/LH encompasses arteriosclerotic, arteriolosclerotic, lipohyalinotic, and fibrohyalinotic changes in small meningeal and parenchymal brain vessels (11). It was noted whether or not a given region exhibited AS/LH-related lesions regardless of the number and severity of the lesions in this specific area. The same regions studied for the extension of CAA were examined to determine the extension of AS/LH by counting the number of regions in a given brain exhibiting AS/LH changes.

Extension of AS/LH = Number of brain regions exhibiting AS/LH-affected vessels

To summarize the total area of the brain exhibiting altered small vessels, regardless of the etiology, we determined the extension of both CAA and/or AS/LH by counting the number of regions exhibiting CAA- and/or AS/LH-affected vessels.

Extension of small vessel lesions = Number of brain regions exhibiting CCA- and/or AS/LH-affected vessels

Statistical Analysis

The Spearman correlation analysis for ranked data was employed to study whether the extensions of CAA and of AS/LH were correlated with the Aβ phase, NFT stage, and the CDR score. To identify whether the extension of CAA and AS/LH have an independent effect on the degree of dementia, which is not linked through the correlation of the extension of CAA and AS/LH with that of Aβ deposition and/or NFT generation, a partial correlation analysis was conducted by controlling the influence of Aβ and NFT pathologies.

We used one-way ANOVA to test for differences in the extension of CAA and the extension of AS/LH among controls, ADRP cases, and AD cases on the one hand as well as the Aβ phases, the NFT stages, and CDR scores on the other. In the event of multiple testing, a post-hoc correction was calculated by using the Tamhane T2 post-hoc test. The Kruskal-Wallis H test was used to identify differences among ranked variables such as CDR score, Aβ phases, and NFT stages.

In order to examine the role of cerebrovascular infarction and intracerebral hemorrhage in AD, we tested for differences in the presence of cerebrovascular infarction and intracerebral hemorrhage in non-AD and AD cases, in CAA cases, and non-CAA cases with the Fisher exact test and calculated odds-ratios. An association of cerebrovascular infarcts and intracerebral hemorrhage with the extension of CAA and AS/LH was tested with one-way ANOVA. To compare the occurrence of intracerebral hemorrhages (including both clinically relevant and irrelevant hemorrhages) with the development of clinically relevant intracerebral hemorrhages in cases with and without CAA and with and without AD we calculated the percentages of all cases with hemorrhages as well as those with clinically relevant intracerebral hemorrhages. The Fisher exact test was used to test whether such differences were statistically relevant. The one-way ANOVA was used to identify differences in the extension of CAA and AS/LH between cases with hemorrhages with and without clinical relevance. To determine the effect of the APOE ε4-allele frequency on the extension of CAA and AS/LH we used one-way ANOVA corrected for multiple testing by using the Tamhane T2-post-hoc test.

RESULTS

The involvement of vessels from different brain regions in CAA as well as in AS/LH followed distinct sequences. This allowed the distinction of 3 stages of CAA and 3 stages of AS/LH (Figs. 1, 2). The extension of both vascular pathologies, CAA and AS/LH, was strongly associated with the development of AD (Table 2).

CAA

The anatomical distribution of CAA-affected vessels allowed the determination of 3 stages of CAA (Figs. 1A, 2A). In stage 1, CAA was restricted to leptomeningeal and cortical vessels of the neocortex (Fig. 3A, B). Stage 2 was characterized by Aβ deposition in vessels of the neocortex, the allocortex (cingulate gyrus, entorhinal cortex, and hippocampus), cerebellum, and the midbrain. In stage 3, CAA-affected vessels were seen in all areas already involved in stage 2 and within the lower brainstem, the basal ganglia, and the thalamus (Fig. 3C). Only one AD patient in CAA stage 3 (case 38) exhibited CAA in the white matter.

TABLE 2
Statistical Analysis

A. Correlation analysis, ANOVA, and non-parametric tests

	CAA-Extension	AS/LH-Extension	SVL-Extension	NFT stage	Aβ phase
Diagnosis	ANOVA: $p < 0.005$	ANOVA: $p < 0.005$	ANOVA: $p < 0.0001$	KW: $p < 0.005$	KW: $p < 0.005$
CDR	$r = 0.57$; ANOVA: $p < 0.005$; PC controlled for Aβ phase $r = 0.164$, $p = 0.28$; PC controlled for NFT stage $r = 0.28$, $p = 0.06$	$r = 0.42$; ANOVA: $p = 0.06$; PC controlled for Aβ phase $r = -0.52$, $p = 0.73$; PC controlled for NFT stage $r = 0.048$, $p = 0.75$	$r = 0.56$; ANOVA: $p < 0.005$; PC controlled for Aβ phase $r = 0.127$, $p = 0.4$; PC controlled for NFT stage $r = 0.229$, $p = 0.126$	$r = 0.65$; KW: $p < 0.0001$	$r = 0.76$; KW: $p < 0.0001$
NFT stage	$r = 0.62$; ANOVA: $p < 0.01$	$r = 0.51$; ANOVA: $p < 0.005$	$r = 0.69$; ANOVA: $p < 0.0001$	—	$r = 0.83$; KW: $p < 0.0001$
Aβ phase	$r = 0.74$; ANOVA: $p < 0.0001$	$r = 0.51$; ANOVA: $p < 0.005$	$r = 0.74$; ANOVA: $p < 0.0001$	$r = 0.83$; KW: $p < 0.0001$	—

B. Association analysis

	AD vs Non-AD	ADRP vs control	Infarction	Hemorrhage	APOE ϵ4 frequency
CAA-Extension	ANOVA: $p < 0.05$	ANOVA: $p < 0.05$	ANOVA: $p = 0.775$	ANOVA: $p = 0.135$	ANOVA: $p < 0.05$
AS/LH-Extension	ANOVA: $p < 0.05$	ANOVA: $p < 0.05$	ANOVA: $p = 0.125$	ANOVA: $p = 0.39$	ANOVA: $p = 0.1$
SVL-Extension	ANOVA: $p < 0.005$	ANOVA: $p < 0.005$	ANOVA: $p = 0.223$	ANOVA: $p = 0.472$	ANOVA: $p < 0.05$

A: Shows the Spearman correlation coefficient for ranked variables (r) between the extension of CAA, AS/LH, and small vessel lesions (SVL) and the CDR score (24), NFT (2), and the Aβ phase (17). The p values presented for these parameters are calculated by one-way ANOVA for differences in interval-scaled extension of CAA, AS/LH, and small vessel lesions and by the Kruskal-Wallis H test for the ranked variables. Partial correlation analysis (PC) is presented for CAA-extension, AS/LH-extension and small vessel lesion-extension controlled either for Aβ phase or NFT. B: Shows the p values of the one-way ANOVA for the extension of CAA, AS/LH, and small vessel lesions (SVL) between AD and non-AD cases; ADRP and control cases; cases with and without cerebral infarction; cases with and without intracerebral hemorrhage; and cases with 1 or 2 APOE ϵ4-alleles and without an APOE ϵ4-allele. A post-hoc correction for multiple testing (Tamhane T2 test) was performed for comparing AD vs non-AD cases, ADRP vs control, and for comparing cases with 0, 1, and 2 APOE ϵ4-alleles. Abbreviations: ANOVA = Analysis of variance; KW = Kruskal-Wallis H test; PC = partial correlation analysis; SVL = small vessel lesions.

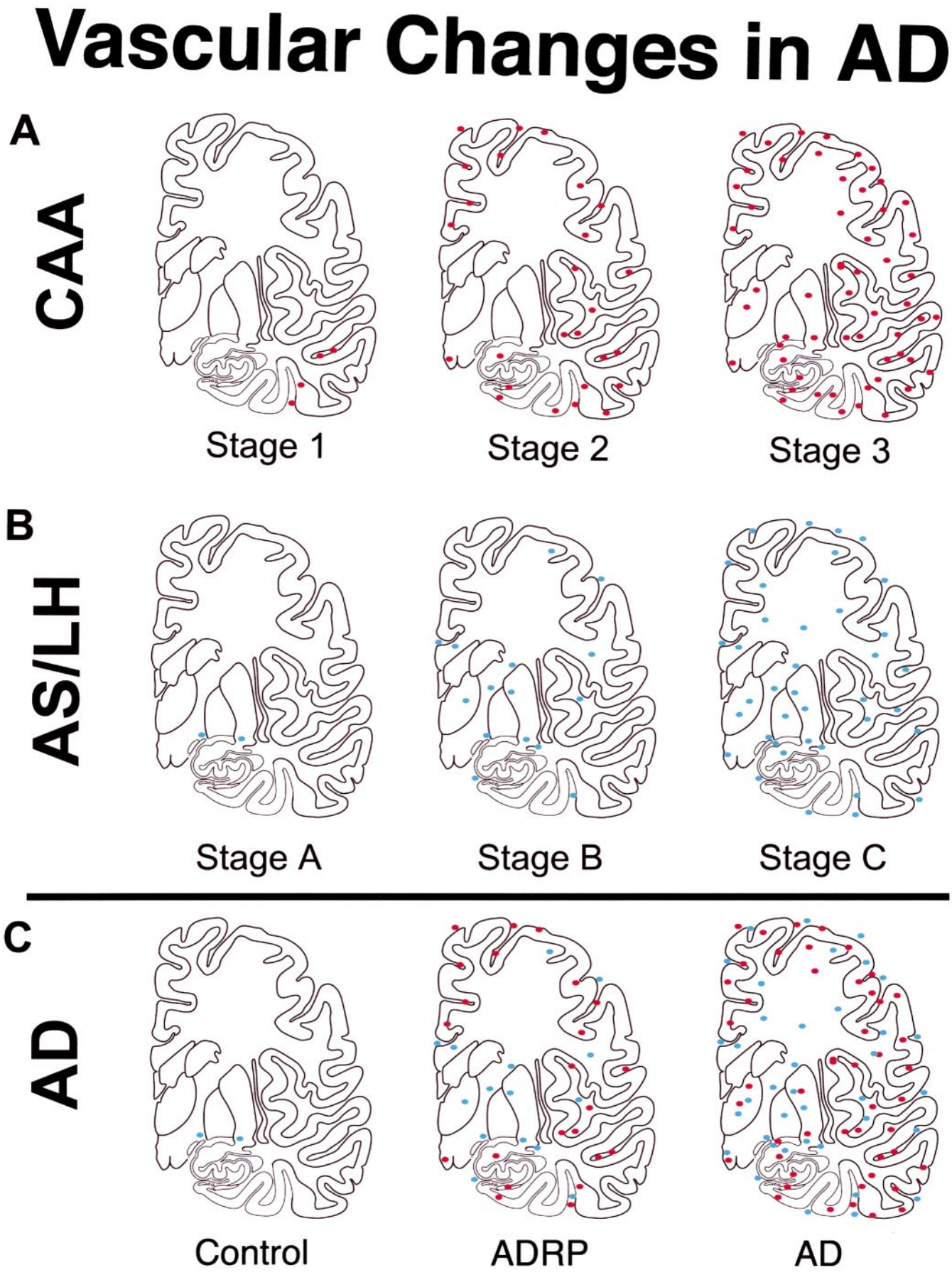

A CAA

Region	Number of affected cases
Occipital neocortex	30
Temporal neocortex	21
Parietal neocortex	20
Frontal neocortex	16
Cerebellum	15
Entorhinal region	14
CA1	12
Cingulate gyrus	11
Dentate gyrus	9
CA4	8
Amygdala	7
Hypothalamus	6
Midbrain	4
Thalamus	3
Basal forebrain	3
Pons*	3
Medulla oblongata*	1
Basal ganglia*	1
Presubicular region	0

no CAA
CAA Stage 1
CAA Stage 2
CAA Stage 3

B AS/LH

Region	Number of affected cases
Occipital neocortex	18
Temporal neocortex	22
Parietal neocortex	11
Frontal neocortex	18
Cerebellum	24
Entorhinal region	4
CA1	0
Cingulate gyrus	23
Dentate gyrus	7
CA4	0
Amygdala	5
Hypothalamus	2
Midbrain	4
Thalamus	24
Basal forebrain	9
Pons	7
Medulla oblongata	8
Basal ganglia	42
Presubicular region	0

no AS/LH
AS/LH stage A
AS/LH stage B
AS/LH stage C

Fig. 2. Distribution of CAA **(A)** and AS/LH **(B)**. **A:** The boxes labeled in black represent the regions exhibiting CAA in CAA stage 1, the regions in dark gray are those becoming involved in CAA stage 2, and those in light gray in CAA stage 3. Regions marked by an asterisk exhibit CAA only in AD cases (*). Regions marked in white did not show CAA-affected vessels. **B:** Regions being involved in AS/LH stage A are labeled in black, those involved in AS/LH stage B in dark gray, and those in stage C in light gray. In the cortical areas, AS/LH changes are almost exclusively located in the leptomeninges and in the white matter. Only in single cases do larger cortical arteries exhibit slight AS/LH changes. The presence of AS/LH changes in the entorhinal cortex, the dentate gyrus, and the amygdala is variable and seen in some AS/LH stage B and C cases, whereas other cases even in stage C do not exhibit such changes. Note that AS/LH exhibits a different pattern of regional involvement in vessel pathology than CAA. Regions marked in white did not exhibit AS/LH lesions.

←

Fig. 1. Schematic representation of stages in the distribution of vascular pathologies in a coronary section through the human brain at the level of the basal ganglia **(A, B)** and their relation to AD **(C)**. **A:** The stages of CAA. CAA changes are indicated in red. The first stage of CAA shows vascular Aβ deposits only in a few neocortical areas and involves leptomeningeal and cortical vessels. Stage 2 is characterized by additional vascular Aβ in the hippocampus, amygdala, hypothalamus, midbrain, and in the cerebellum (midbrain and cerebellum are not shown in this figure). In stage 3, CAA is also seen in vessels of the basal ganglia, the thalamus, and the basal forebrain. Aβ deposition in the lower brainstem, another feature of CAA stage 3, is not depicted. **B:** The stages of AS/LH. AS/LH changes are highlighted in blue. First, in stage A, AS/LH changes can be observed in the basal ganglia and in the deep white matter. Stage B is characterized by additional AS/LH in the cortical and cerebellar leptomeninges and in the thalamus. In the final stage of AS/LH (stage C), AS/LH changes expand into vessels of the hypothalamus and the brainstem (cerebellum and brainstem are not shown in this figure). **C:** A summary of the CAA (red) and AS/LH (blue) pathologies. In controls without AD-related pathology, CAA is absent and AS/LH is restricted to single vessels in the deep white matter or the basal ganglia. In ADRP, CAA affects the occipital, temporal and frontal cortex, and occasionally other neocortical and allocortical areas, whereas AS/LH is restricted to vessels of the basal ganglia, the deep white matter, the thalamus, and the leptomeninges. AD cases exhibit CAA most frequently in all cortical fields, often in the cerebellum and less frequently in the thalamus, the basal ganglia, the basal forebrain, and the lower brainstem. In the AD brain, AS/LH regularly occurs in the basal ganglia, the deep and peripheral white matter, the thalamus, the hypothalamus, the amygdala, and the leptomeningeal vessels.

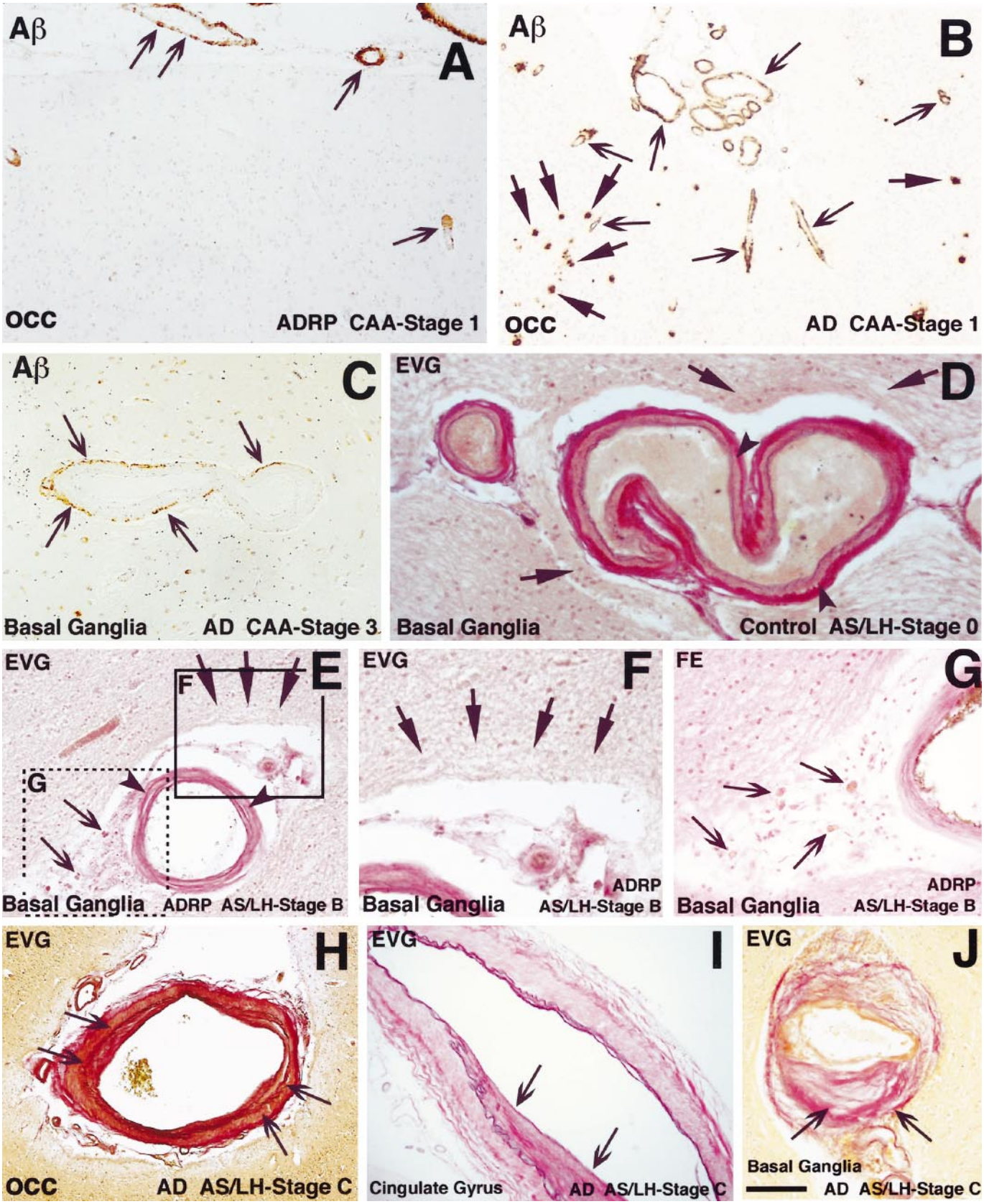

Vascular Aβ deposition was accompanied by parenchymal Aβ plaques. In most instances, all regions exhibiting CAA also showed Aβ plaques. In only a few cases was CAA seen in the absence of Aβ plaques in a given area, although Aβ plaques prevailed in other regions. Such anatomical structures showing vascular Aβ deposition in the absence of parenchymal Aβ were the dentate gyrus (22% of cases with vascular Aβ deposits in the dentate gyrus), CA1 (8% of cases with vascular Aβ deposits in CA1), CA4 (37.5% of cases with vascular Aβ deposits in CA4), the cingulate gyrus (9% of cases with vascular Aβ deposits in the cingulate gyrus), the parietal neocortex (5% of cases with vascular Aβ deposits in the parietal neocortex), the pons (33% of cases with vascular Aβ deposits in the pons), and the cerebellum (20% of cases with vascular Aβ deposits in the cerebellum). The other regions studied exhibited CAA only in the presence of Aβ plaques. Two demented and 11 nondemented cases exhibited Aβ plaques in the complete absence of CAA. Both demented cases free of CAA showed the morphological pattern of argyrophilic grain disease in addition to AD-related lesions and, therefore, did not match the diagnosis of pure AD.

The sequences of extension of CAA and Aβ plaques both started in the neocortex and then spread into the allocortex. Afterwards, Aβ plaques occurred in the basal ganglia before the cerebellum was involved (17). In contrast, the basal ganglia were one of the last regions to develop vascular Aβ, while CAA was already present in the cerebellar vessels. Cases exhibiting capillary Aβ deposits indicative for an APOE ε4-associated type of CAA (29) were found in all stages of CAA. There was no local association between CAA and NFTs. For example, NFTs were seen in Brodmann area 17 in only 2 NFT stage VI cases whereas 30 brains showed CAA in this region.

AS/LH

The hierarchical involvement of different brain regions with AS/LH vessels allowed the distinction of 3 stages of AS/LH (Fig. 1B). Stage A was characterized by AS/LH either in the basal ganglia or in the cerebral deep white matter. Stage B cases exhibited AS/LH changes in the basal ganglia, the deep white matter of the cerebrum and cerebellum, the thalamus, and in the leptomeningeal vessels of the cerebral and cerebellar cortex. Stage C cases showed, in addition to the vascular changes described for stage B, AS/LH changes in the small leptomeningeal and parenchymal vessels of the brainstem and the hypothalamus. Atherosclerosis of large brain vessels such as the vertebral, basilar, anterior, middle and posterior cerebral arteries, and the internal carotid artery was ignored for AS/LH staging.

The severity of AS/LH lesions ranged from splitting of the internal elastic lamina (Fig. 3E, H), initial fibrotic degeneration, moderate numbers of perivascular lipid-containing macrophages (Fig. 3G, small arrows), and slightly enlarged perivascular cavities to a complete loss of smooth muscle cells, fibrosis of the vessel wall (Fig. 3I, J), aneurysmatic degeneration, fibrohyalinosis of white matter vessels with perivascular loss of myelin, axons, and oligodendrocytes, as well as large perivascular cavities (Fig. 3E, F, large arrows). A negative Prussian blue staining reaction distinguished lipid-containing macrophages from siderophages (Fig. 3G). All of these changes were seen in vessels of AD cases as well as of ADRP cases. Splitting of the internal elastic lamina and arteriosclerotic plaques were predominantly observed in small vessels of the leptomeninges (Fig. 3H, I), whereas fibrohyalinotic and lipohyalinotic changes were found predominantly in vessels of the basal ganglia, white matter, and the thalamus (Fig. 3E–G, J).

←

Fig. 3. Small vessel changes in AD cases and in nondemented individuals (ADRP cases and controls). CAA starts with few leptomeningeal and cortical vascular Aβ deposits (arrows) in neocortical areas in ADRP cases **(A)**. Note that no Aβ plaques are associated with the vascular Aβ deposits in this area **(A)**. Vascular Aβ deposition in the leptomeningeal and cortical vessels (arrows) in AD concurrently occurs with Aβ plaques in the vicinity of CAA-affected vessels (bold arrows) **(B)**. In AD cases with severe CAA, vascular Aβ deposits also occur in vessels of the basal ganglia **(C)**. AS/LH changes are often absent in controls lacking Aβ deposits and NFTs **(D)**. In cases with AD-related pathology, even if they are nondemented, AS/LH occurs in vessels of the basal ganglia **(E–G)**. These vessels exhibit focal loss of smooth muscle cells, which are replaced by fibrotic material stained in red (arrowheads in **E**). There is also splitting of the internal elastic lamina. **G:** Prussian blue negative, lipid-containing macrophages in the perivascular space in a parallel section of **(E)** stained with the Prussian blue method. The perivascular space around the affected vessel is widened **(E)**. The enlargement of panel **(E)** depicts that the adjacent brain parenchyma exhibits focal loss of myelin, axons, and oligodendrocytes compared to controls (bold arrows in **E, F**). For comparison, panel **(D)** depicts the brain parenchyma adjacent to an unaffected control vessel (bold arrows). In AD cases, severe AS/LH changes can regularly be observed **(H–J)**. Arteriosclerotic changes are seen in the leptomeninges **(H, I)**. The artery depicted in panel **(H)** shows only minor arteriosclerotic changes with splitting of the internal elastic lamina and intimal proliferation (arrows), whereas the vessel illustrated in panel **(I)** exhibits an arteriosclerotic plaque (arrows). The artery depicted in panel **(J)** represents severe AS/LH of an intracerebral vessel with a complete loss of smooth muscle cells in the media and severe fibrosis. Calibration bar: **A, J:** 90 μm; **B, C, I:** 150 μm; **D, F, G:** 65 μm; **E:** 110 mm; **G:** 65 mm; **H:** 250 μm. Staining method: **A–C:** Immunohistochemistry with antibodies directed against $A\beta_{17-24}$ (Aβ); **D–F, H–J:** Elastica van Gieson staining method (EVG); **G:** Prussian blue iron staining method (FE). Cases: 1 **(D)**, 9 **(A)**, 34 **(B)**, 38 **(C)**, 41 **(H–J)**, and 50 **(E–G)**.

AS/LH occurred in the absence of Aβ and NFT pathology in single white matter vessels. With increasing extension of AS/LH, NFTs and Aβ deposits were observed in an increasing number of regions. NFTs and parenchymal Aβ plaques were predominantly seen in the gray matter whereas AS/LH changes were primarily located in large white matter vessels, in vessels of the basal ganglia and the leptomeninges, but not in cortical vessels. Vascular Aβ deposition was predominantly seen in blood vessels not affected by AS/LH. Only few leptomeningeal vessels in cases with severe AS/LH and CAA exhibited both arteriosclerotic changes and Aβ deposition in the vessel wall.

Together, small vessel lesions due to CAA and/or AS/LH occurred in a mean of 10 different regions in the AD brain (Fig. 4A). These regions included the entire allo- and neocortex, the cerebral white matter, the basal ganglia, and the thalamus (Fig. 1). Atherosclerotic plaques were seen in the large vessels of the circle of Willis in 25% of the controls, 88% of the ADRP, and 100% of the AD cases.

Statistical Analysis (Fig. 4; Table 2)

Validity of Stages: The validity of the CAA stages was confirmed by demonstrating that the number of CAA-affected brain regions as represented by the extension of CAA increases with the stage of CAA (Kruskal-Wallis H test: $p < 0.0001$). Likewise, the AS/LH stages were validated by a growing number of regions exhibiting AS/LH changes as represented by the extension of AS/LH (Kruskal-Wallis H test: $p < 0.0001$). Since the stages of CAA and AS/LH were ranked variables, we used the interval-scaled extension of CAA and AS/LH for further statistical analysis.

CAA: AD cases showed a higher extension of CAA than ADRP and control cases (one-way ANOVA corrected for multiple testing: $p < 0.05$; Fig. 4A). In control cases, the extension of CAA was lower compared to ADRP and AD cases (one-way ANOVA corrected for multiple testing: $p < 0.05$). The extension of CAA correlated with the degree of dementia as determined by the CDR scores (one-way ANOVA: $p < 0.005$; Spearman correlation, $r = 0.57$; Fig. 4B), the stage of Aβ deposition in the human brain as shown by the Aβ phases (one-way ANOVA: $p < 0.0001$; Spearman correlation, $r = 0.74$; Fig. 4C), and with the NFT stage (one-way ANOVA; Spearman correlation, $r = 0.62$; Fig. 4D). Controlling for Aβ phase and NFT stage, partial correlation between the extension of CAA and the CDR score revealed no significant independent relationship (controlling for Aβ: $r = 0.17$, $p = 0.277$; controlling for NFT: $r = 0.28$, $p = 0.059$), indicating that the correlation between the extension of CAA and the CDR score as seen with the Spearman correlation analysis is linked through Aβ phase and/or NFT stage. The extension of CAA also correlated with the extension of AS/LH (one-way ANOVA: $p < 0.05$; Spearman correlation, $r = 0.37$). The stages of CAA correlated with the extension of CAA and AS/LH, the NFT stage, and the Aβ phase (Table 2).

AS/LH: The extension of AS/LH was higher in AD cases compared to ADRP cases and controls (one-way ANOVA corrected for multiple testing: $p < 0.05$; Fig. 4A). ADRP cases showed a higher extension of AS/LH compared to controls without any AD-related pathology (one-way ANOVA corrected for multiple testing: $p < 0.05$; Fig. 4A). The extension of AS/LH increased with the CDR score (one-way ANOVA: $p = 0.06$; Spearman correlation, $r = 0.42$; Fig. 4B), the Aβ phase (one-way ANOVA: $p < 0.005$; Spearman correlation, $r = 0.51$; Fig. 4C), and with the NFT stage (one-way ANOVA: $p < 0.005$; Spearman correlation, $r = 0.51$; Fig. 4D). Partial correlation analysis between the extension of AS/LH and the degree of dementia controlled for Aβ phase and NFT stage revealed no independent correlation (controlling for Aβ: $r = 0.06$, $p = 0.67$; controlling for NFT: $r = 0.13$, $p = 0.393$). In so doing, the correlation between the extension of AS/LH and the CDR score as seen in the Spearman correlation analysis is linked through Aβ phase and/or NFT stage. The extension of AS/LH increased up to and including NFT stage V and decreased slightly in NFT stage VI (Fig. 4D). The stages of AS/LH correlated with the NFT stage and the phase of β-amyloidosis (Table 2).

Total Small Vessel Lesions due to CAA and AS/LH: The number of brain regions with small vessel pathology regardless of their etiology was summarized as extension of small vessel lesions and this parameter was higher in AD cases than in ADRP and controls (one-way ANOVA corrected for multiple testing: $p < 0.005$; Fig. 4A; Table 2). The extension of small vessel lesions also correlated with the CDR score (one-way ANOVA: $p < 0.005$; Spearman correlation, $r = 0.56$; Fig. 4B; Table 2), the Aβ phase (one-way ANOVA: $p < 0,0001$; Spearman correlation, $r = 0.74$; Fig. 4C; Table 2), and with the NFT stage (one-way ANOVA: $p < 0.0001$; Spearman correlation, $r = 0.69$; Fig. 4D; Table 2). Partial correlation analysis controlled for Aβ phase and NFT stage revealed no independent correlation between the extension of small vessel lesions and the CDR score (partial correlation controlling for Aβ phase: $r = 0.127$, $p = 0.401$; controlling for NFT stage: $r = 0.229$, $p = 0.126$), indicating that the correlation between the extension of small vessel lesions and the CDR score as seen in the Spearman correlation analysis is one through Aβ phase and/or NFT stage. A relationship was also noted for CAA stage and AS/LH stage and the extension of small vessel lesions (Table 2).

APOE: The extension of CAA was higher in carriers of the APOE ε4-allele than in non-carriers (one-way ANOVA corrected for multiple testing: $p < 0.05$). Carriers

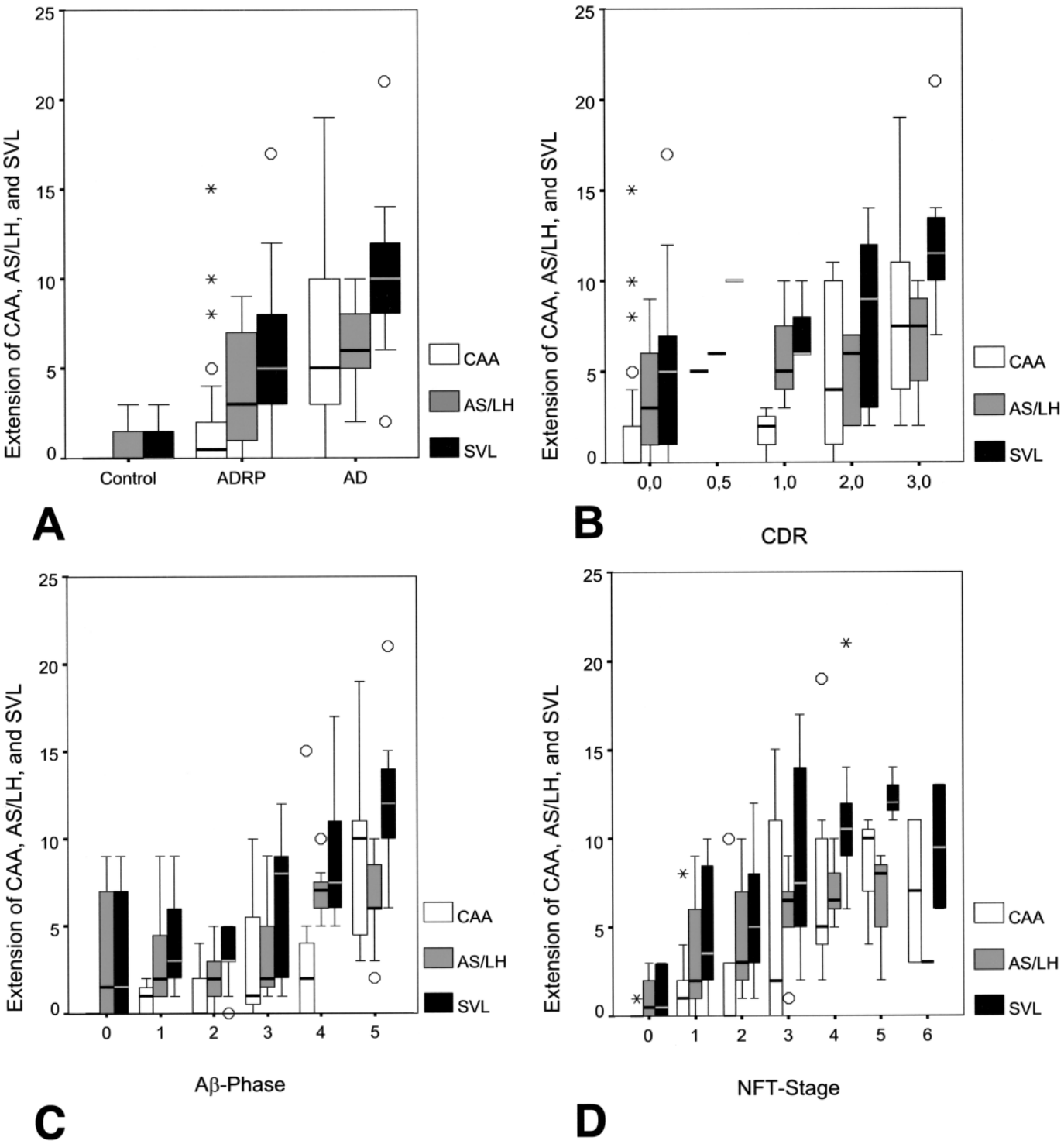

Fig. 4. **A:** Box and whisker plots illustrating ranges and medians of the extension of CAA (white boxes), AS/LH (gray boxes), and of small vessel changes (SVL, black boxes) by different categories. Diagram **(A)** shows ranges and medians of the extension of CAA, AS/LH, and of small vessel lesions in controls without NFTs and Aβ deposits, ADRP, and AD cases. AD cases exhibit CAA, AS/LH, and small vessel lesions in more regions than in ADRP and control cases. ADRP cases show CAA, AS/LH, and small vessel lesions in more regions than controls. Diagrams **(B–D)** depict ranges and the medians of the extension of CAA, AS/LH, and of small vessel lesions by CDR score **(B)**, Aβ phase **(C)**, and NFT stage **(D)**. Demented cases with CDR scores ranging between 0.5 (representing mild cognitive impairment) and 3 (representing severe dementia) exhibit a higher extension of CAA, AS/LH and small vessel lesions compared to nondemented cases with a CDR score of 0 (**B**). The extension of CAA, AS/LH, and SVL increases with the expanding distribution of Aβ deposits **(C)**. There is an increase in the extension of CAA, AS/LH, and small vessel lesions up to and including NFT V followed by a slight decrease in NFT VI cases **(D)**. The extension of CAA, AS/LH, and small vessel lesions represents the number of regions showing vessels involved either in CAA, AS/LH, or in small vessel lesions. The boxes encompass 50% of the cases, the bar within the boxes displays the median, and the ranges cover all cases except those with striking deviation. Cases with values in 1.5- to 3-fold distance from the boxes are indicated with a circle. Extreme values are those more than 3-fold distant from the box and are indicated with an asterisk.

of an APOE ε4-allele showed a slightly greater extension of AS/LH than non-APOE ε4 carriers but this trend failed to reach significance (one-way ANOVA corrected for multiple testing: $p = 0.085$). The extension of small vessel lesions was higher in carriers of the APOE ε4-allele compared to non-carriers (one-way ANOVA corrected for multiple testing: $p < 0.05$).

Infarction: Cerebral infarction was found in 70.6% of the AD cases but in only 35.5% of the ADRP and control cases (odds ratio: 4.1, confidence interval: 1.152–14.923; Fisher exact test: $p < 0.05$). 48.5% of the cases with CAA and 42.1% of cases without CAA showed cerebral infarction (Fisher exact test: $p = 0.5455$). The extension of CAA was higher in cases with cerebral infarction than in those without (one-way ANOVA: $p < 0.05$; Table 2). Cases with cerebral infarction also exhibited a slightly greater extension of AS/LH than cases without cerebral infarction (one-way ANOVA: $p = 0.1$) and a significantly greater extension of small vessel lesions due to CAA and AS/LH (one-way ANOVA: $p < 0.05$).

Intracerebral Hemorrhage: Intracerebral hemorrhagic lesions at both the macroscopical and microscopical level occurred in 17.7% of AD and in 29.0% of ADRP and controls (Fisher exact test: $p = 0.4923$), whereas large clinically relevant intracerebral hemorrhages were seen in 11.8% of the AD but only in 7.7% of the nondemented cases (Fisher exact test: $p = 1$).

Intracerebral hemorrhage was detected histopathologically in 18.2% of cases with CAA and in 36.8% of the cases without CAA (Fisher exact test: $p = 0.1866$), whereas hemorrhages with clinical relevance occurred in 9.1% of the CAA cases and in 10.5% of cases without CAA (Fisher exact test: $p = 1$). This indicates that 50% of the hemorrhages occurring in CAA cases became clinically relevant compared to 29% of the hemorrhages in non-CAA cases. The extension of CAA did not show an effect on the prevalence of clinically relevant hemorrhage in comparison to silent hemorrhages (one-way ANOVA: $p = 0.524$). The extension of AS/LH did not differ between cases with and without intracerebral hemorrhage (ANOVA: $p = 0.39$; Table 2). Although the extension of AS/LH was slightly higher in cases with clinically relevant intracerebral hemorrhages than in those with clinically silent hemorrhages, this parameter failed to reach significance (one-way ANOVA: $p < 0.284$).

DISCUSSION

In this study we show that the extension of CAA and AS/LH is increased in AD cases. Although it is well-known that AS/LH lesions occur in the presence as well as in the absence of AD (5, 11, 16), our data indicate that widespread small vessel lesions due to both CAA and AS/LH may play a critical role in the development of AD. This hypothesis is supported by our finding of a strong correlation between the extension of small vessel lesions with the CDR score as well as with both histopathological hallmarks of AD, NFTs, and Aβ deposits. The relationship between the extension of CAA and AS/LH and the degree of dementia is presumably not an independent one. Partial correlation analysis suggests that these vascular changes occur in concert with AD-related Aβ deposition and NFT pathology. Thus, small vessel changes due to CAA and AS/LH appear to be an integral component of AD-related pathology. The fact that nondemented ADRP cases with early stages of NFT and Aβ pathology show a higher extension of small vessel lesions compared to controls free of Aβ and NFTs is also compatible with an involvement of small vessel changes in the pathogenesis of AD. Hence, our results confirm an association between AD and CAA (7–9, 23, 32) as well as AS/LH (5, 7, 10, 16). The findings presented here extend the present knowledge of AD-related vascular pathology insofar as we show that the extension of small vessel changes throughout the entire brain is associated with the development of AD-related Aβ and NFT pathology and with the development of cognitive deficits (Fig. 4). Our results suggest that small vessel changes represent an important histopathological component of AD and may contribute to neurodegeneration in late-onset AD.

To further characterize the role of small vessel lesions for the deposition of Aβ and for the generation of NFTs, we analyzed the anatomical distribution of CAA and AS/LH and its relation to parenchymal Aβ deposition and NFT generation. Our results show that CAA and AS/LH develop in the different brain areas in a distinct hierarchical sequence that can be described by 3 stages for CAA and AS/LH (Fig. 4). The development of CAA starts in stage 1 in leptomeningeal and cortical vessels of the occipital, parietal, temporal and frontal neocortex, expands in stage 2 into allocortical and cerebellar regions, and finally involves the basal ganglia, the white matter, the thalamus, and the lower brainstem in stage 3. On the other hand, AS/LH commences in the basal ganglia and the deep white matter (11, 33) (stage A), expands into the vasculature of the cortical leptomeninges, the thalamus, and the cerebellum (stage B), and finally affects small leptomeningeal and parenchymal brainstem vessels (stage C). Both the stages of CAA and those of AS/LH correlated with the NFT stages and Aβ phases and were higher in AD cases than in ADRP and controls.

Initial Aβ deposits in the cortical vessels occur in parallel with the onset of parenchymal Aβ deposition in this area (17). Subsequently, vascular Aβ pathology expands into vessels of the allocortex and the cerebellum before vascular Aβ deposits occur in the thalamus and the basal ganglia. This sequence is different from that seen for parenchymal Aβ plaques. Here, the thalamus and the basal ganglia exhibit Aβ deposits before Aβ plaques occur in

the cerebellum (17). Despite these differences in the sequences of vascular and parenchymal Aβ deposition, vascular Aβ-changes were strongly associated with the parallel development of Aβ plaques in the same region, indicating a close local relationship between parenchymal and vascular Aβ deposition. The late involvement of thalamic and basal ganglia vessels in comparison to the development of Aβ plaques in this region may point to a lower susceptibility for vascular Aβ deposition in these areas as compared to the surrounding brain parenchyma. Several mechanisms may account for a reduced susceptibility for CAA: 1) Perivascular spaces in the basal ganglia differ in their anatomy from those in the cortex (34). 2) Branches of the middle cerebral artery in the basal ganglia and the thalamus that contain central channels of the periarterial pathways for interstitial fluid drainage (35–37) accumulate extracellular Aβ only in the event that the periarterial channels in the distal branches of these arteries are already filled with Aβ deposits. 3) Preexisting AS/LH changes of these vessels may reduce the interstitial fluid drainage via periarterial pathways resulting in deposition of Aβ in distal parts of the periarterial pathways. The third explanation is supported by our finding that AS/LH changes occur early in the development of AD within the major branches of the middle cerebral artery, for example, in the basal ganglia and in the deep white matter. Initial AS/LH of central brain arteries can also be discussed as a possible mechanism for initial parenchymal Aβ deposition as a consequence of impaired Aβ clearance from the brain parenchyma along periarterial channels (38). The local pattern of CAA is different from that of NFT generation and may not be directly linked.

The stages of AS/LH show that these small vessel changes also occur in a sequence in which vessels of distinct brain regions are involved. It appears that proximal arteries in the basal ganglia and in the deep white matter are particularly susceptible to AS/LH whereas smaller distal arteries, such as cortical arteries, less frequently exhibit AS/LH pathology. The hierarchical involvement of distinct brain regions in small vessel lesions due to arteriosclerosis, arteriolosclerosis, fibrohyalinosis, and lipohyalinosis argues in favor of summarizing these vascular changes as AS/LH.

In our sample, cerebral infarction was more frequently found in AD cases as compared to ADRP and controls. Since only a marginal significance was noted concerning the association between AD and cerebral infarction, a separate study in a larger series of cases appears warranted. A recent report supports an association between cerebral infarction and AD (39). On the other hand, 29.4% of our AD cases did not show any cerebral infarction. Since we show that AD brains without cerebral infarction also contain a significant amount of small vessel changes, one may conclude that small vessel lesions play a pathogenetic role in AD independent of cerebral infarction. Impaired perfusion of the affected microvasculature leads to alterations in the cerebral blood flow with hypoperfusion of the brain parenchyma as shown in magnetic resonance imaging and single photon emission computed tomography studies in AD patients (40–44) and in animal experiments (45, 46). Although there is no local relationship between AS/LH and the generation of NFTs, it is tempting to speculate that cortical hypoperfusion due to AS/LH in the central branches of the middle cerebral artery induces hypoxia and leads to τ-protein dephosphorylation and translocation of this protein into the perikaryon (47) while hypoperfusion-induced excitotoxicity supports abnormal phosphorylation of the τ-protein (48). Such a scenario may represent a possible link between vascular changes and τ-protein function and phosphorylation status.

CAA and AS/LH may support the development of larger hemorrhages that become clinically relevant. Arguments favoring this view are 1) Intracerebral hemorrhage occurs in cases with and without CAA and 2) hemorrhages become more frequently clinically relevant in CAA cases, although in our sample small clinically silent hemorrhages were more frequently seen in CAA cases. Since our results fail to reach significance, further studies are required to clarify the mechanisms of CAA- and/or AS/LH-induced intracerebral hemorrhage.

Current consensus criteria recommend the diagnosis of AD in cases with NFT stages V and VI and a high score of neuritic plaques. Cases with NFT stages III and IV and moderate numbers of neuritic plaques allow the diagnosis of AD in the event that other causes for dementia can be excluded (25). A diagnosis of vascular dementia is recommended in patients with cerebral infarction and vessel lesions due to AS/LH, atherosclerosis, and other vascular disorders in the absence of significant AD-related pathology (49). Cases with an overlapping pattern of vascular and AD lesions are often categorized as mixed dementia or as AD with cerebrovascular disease (5, 49). Our finding that an increased extension of small vessel lesions in the brain is a regular histopathological feature of sporadic late-onset AD in contrast to ADRP and controls raises an obvious problem in the differential diagnosis between vascular dementia, AD, and mixed dementia. The detection of abnormalities in cerebral perfusion and of cerebral infarction is not suited to distinguish AD from vascular dementia (39, 41, 42). This notion is supported by a recent study indicating that small cerebral infarcts do not increase the level of dementia in AD (50), whereas larger infarcts may alter cognitive function (51), as well as infarcts in patients with low levels of AD-related pathology (52). Therefore, our data together with those of other authors favor the hypothesis that small cerebral infarcts in late-onset AD cases can be interpreted

as a complication of AD-related small vessel lesions rather than as evidence for non-AD-related vascular events.

Our results suggest that AS/LH in the brain may serve as a potential target for the treatment of AD. This target also argues in favor of using statins in late-onset AD patients not only for their Aβ-lowering effects (53, 54).

ACKNOWLEDGMENTS

The authors gratefully acknowledge the technical assistance of U. Enderlein, H. Korff and U. Klatt and the help of Mrs. K. Gierga in editing the manuscript.

REFERENCES

1. Alzheimer A. Ueber eine eigenartige Erkrankung der Hirnrinde. Allg Zschr Psych 1907;64:146–48
2. Braak H, Braak E. Neuropathological stageing of Alzheimer-related changes. Acta Neuropathol 1991;82:239–59
3. Esiri MM, Hyman BT, Beyreuther K, et al. Ageing and dementia. In: Lantos PL, ed. Greenfields neuropathology, 6th Edition. London: Arnold, 1997:153–233
4. Masters CL, Simms G, Weinman NA, et al. Amyloid plaque core protein in Alzheimer disease and Down syndrome. Proc Natl Acad Sci U S A 1985;82:4245–49
5. Jellinger KA. Alzheimer disease and cerebrovascular pathology: An update. J Neural Transm 2002;109:813–36
6. de la Torre JC. Alzheimer disease as a vascular disorder: Nosological evidence. Stroke 2002;33:1152–62
7. Kalaria RN, Ballard C. Overlap between pathology of Alzheimer disease and vascular dementia. Alzheimer Dis Assoc Disord 1999; 13Suppl 3:S115–23
8. Joachim CL, Morris JH, Selkoe DJ. Clinically diagnosed Alzheimer's disease: Autopsy results in 150 cases. Ann Neurol 1988;24: 50–56
9. Mandybur TI. Cerebral amyloid angiopathy: The vascular pathology and complications. J Neuropathol Exp Neurol 1986;45:79–90
10. Skoog I, Kalaria RN, Breteler MM. Vascular factors and Alzheimer disease. Alzheimer Dis Assoc Disord 1999;13Suppl 3:S106–14
11. Vinters HV, Ellis WG, Zarow C, et al. Neuropathologic substrates of ischemic vascular dementia. J Neuropathol Exp Neurol 2000;59: 931–45
12. Esiri MM, Wilcock GK, Morris JH. Neuropathological assessment of the lesions of significance in vascular dementia. J Neurol Neurosurg Psychiatry 1997;63:749–53
13. Bergeron C, Ranalli PJ, Miceli PN. Amyloid angiopathy in Alzheimer's disease. Can J Neurol Sci 1987;14:564–69
14. Vinters HV. Cerebral amyloid angiopathy. In: Yatsu FM. Stroke. Pathophysiology, diagnosis and management. New York: Churchill Livingstone, 1992:821–58
15. Yamada M, Tsukagoshi H, Otomo E, et al. Cerebral amyloid angiopathy in the aged. J Neurol 1987;234:371–76
16. Brun A, Englund E. A white matter disorder in dementia of the Alzheimer type: A pathoanatomical study. Ann Neurol 1986;19: 253–62
17. Thal DR, Rüb U, Orantes M, et al. Phases of Abeta-deposition in the human brain and its relevance for the development of AD. Neurology 2002;58:1791–1800
18. Thal DR, Holzer M, Rüb U, et al. Alzheimer-related tau-pathology in the perforant path target zone and in the hippocampal stratum oriens and radiatum correlates with onset and degree of dementia. Exp Neurol 2000;163:98–110
19. Arnold SE, Hyman BT, Flory J, et al. The topographical and neuroanatomical distribution of neurofibrillary tangles and neuritic plaques in the cerebral cortex of patients with Alzheimer's disease. Cereb Cortex 1991;1:103–16
20. Bancher C, Braak H, Fischer P, et al. Neuropathological staging of Alzheimer lesions and intellectual status in Alzheimer's and Parkinson's disease patients. Neurosci Lett 1993;162:179–82
21. Gomez-Isla T, Price JL, McKeel DW Jr., et al. Profound loss of layer II entorhinal cortex neurons occurs in very mild Alzheimer's disease. J Neurosci 1996;16:4491–4500
22. Thal DR, Rüb U, Schultz C, et al. Sequence of Abeta-protein deposition in the human medial temporal lobe. J Neuropathol Exp Neurol 2000;59:733–48
23. Pfeifer LA, White LR, Ross GW, et al. Cerebral amyloid angiopathy and cognitive function: The HAAS autopsy study. Neurology 2002;58:1629–34
24. Hughes CP, Berg L, Danziger WL, et al. A new clinical scale for the staging of dementia. Br J Psychiatry 1982;140:566–72
25. The National Institute on Aging. Consensus recommendations for the postmortem diagnosis of Alzheimer's disease. The National Institute on Aging, and Reagan Institute Working Group on Diagnostic Criteria for the Neuropathological Assessment of Alzheimer's Disease. Neurobiol Aging 1997;18:S1–S2
26. Braak H, Braak E. Demonstration of amyloid deposits and neurofibrillary changes in whole brain sections. Brain Pathol 1991;1: 213–16
27. Wenham PR, Price WH, Blandell G. Apolipoprotein E genotyping by one-stage PCR. Lancet 1991;337:1158–59
28. Ghebremedhin E, Braak H, Braak E, et al. Improved method facilitates reliable APOE genotyping of genomic DNA extracted from formaldehyde-fixed pathology specimens. J Neurosci Methods 1998;79:229–31
29. Thal DR, Ghebremedhin E, Rüb U, et al. Two types of sporadic cerebral amyloid angiopathy. J Neuropathol Exp Neurol 2002;61: 282–93
30. Iwatsubo T, Saido TC, Mann DM, et al. Full-length amyloid-beta (1–42(43) and amino-terminally modified and truncated amyloid-beta 42(43) deposit in diffuse plaques. Am J Pathol 1996;149: 1823–30
31. Kim KS, Miller DL, Sapienza VJ, et al. Production and characterization of monoclonal antibodies reactive to synthetic cerebrovascular amyloid peptide. Neurosci Res Commun 1988;2:121–30
32. Vinters HV, Wang ZZ, Secor DL. Brain parenchymal and microvascular amyloid in Alzheimer's disease. Brain Pathol 1996;6:179–95
33. Kalimo H, Kaste M, Haltia M. Vascular diseases. In: Lantos PL. Greenfield's neuropathology, 6th Edition. London: Arnold, 1997: 315–96
34. Pollock H, Hutchings M, Weller RO, et al. Perivascular spaces in the basal ganglia of the human brain: Their relationship to lacunes. J Anat 1997;191(Pt 3):337–46
35. Kida S, Pantazis A, Weller RO. CSF drains directly from the subarachnoid space into nasal lymphatics in the rat. Anatomy, histology and immunological significance. Neuropathol Appl Neurobiol 1993;19:480–88
36. Weller RO, Massey A, Newman TA, et al. Cerebral amyloid angiopathy: Amyloid beta accumulates in putative interstitial fluid drainage pathways in Alzheimer's disease. Am J Pathol 1998;153: 725–33
37. Weller RO. Pathology of cerebrospinal fluid and interstitial fluid of the CNS: Significance for Alzheimer disease, prion disorders and multiple sclerosis. J Neuropathol Exp Neurol 1998;57:885–94
38. Preston SD, Steart PV, Wilkinson A, et al. Capillary and arterial cerebral amyloid angiopathy in Alzheimer's disease: Defining the perivascular route for the elimination of amyloid beta from the human brain. Neuropathol Appl Neurobiol 2003;29:106–17
39. Jellinger KA, Attems J. Incidence of cerebrovascular lesions in Alzheimer's disease: A postmortem study. Acta Neuropathol (Berl) 2003;105:14–17
40. Johnson KA, Jones K, Holman BL, et al. Preclinical prediction of Alzheimer's disease using SPECT. Neurology 1998;50:1563–71

41. Jagust W, Thisted R, Devous MD Sr., et al. SPECT perfusion imaging in the diagnosis of Alzheimer's disease: A clinical-pathologic study. Neurology 2001;56:950–56
42. Kogure D, Matsuda H, Ohnishi T, et al. Longitudinal evaluation of early Alzheimer's disease using brain perfusion SPECT. J Nucl Med 2000;41:1155–62
43. de la Torre JC. Critical threshold cerebral hypoperfusion causes Alzheimer's disease? Acta Neuropathol (Berl) 1999;98:1–8
44. Devous Sr MD. Functional brain imaging in the dementias: Role in early detection, differential diagnosis, and longitudinal studies. Eur J Nucl Med Mol Imaging 2002;29:1685–96
45. De Jong GI, Farkas E, Stienstra CM, et al. Cerebral hypoperfusion yields capillary damage in the hippocampal CA1 area that correlates with spatial memory impairment. Neuroscience 1999;91:203–10
46. Mueggler T, Sturchler-Pierrat C, Baumann D, et al. Compromised hemodynamic response in amyloid precursor protein transgenic mice. J Neurosci 2002;22:7218–24
47. Burkhart KK, Beard DC, Lehman RA, et al. Alterations in tau phosphorylation in rat and human neocortical brain slices following hypoxia and glucose deprivation. Exp Neurol 1998;154:464–72
48. Sautiere PE, Sindou P, Couratier P, et al. Tau antigenic changes induced by glutamate in rat primary culture model: A biochemical approach. Neurosci Lett 1992;140:206–10
49. Roman GC, Tatemichi TK, Erkinjuntti T, et al. Vascular dementia: Diagnostic criteria for research studies. Report of the NINDS-AIREN International Workshop. Neurology 1993;43:250–60
50. Lee JH, Olichney JM, Hansen LA, et al. Small concomitant vascular lesions do not influence rates of cognitive decline in patients with Alzheimer disease. Arch Neurol 2000;57:1474–79
51. Zekry D, Duyckaerts C, Moulias R, et al. Degenerative and vascular lesions of the brain have synergistic effects in dementia of the elderly. Acta Neuropathol (Berl) 2002;103:481–87
52. Esiri MM, Nagy Z, Smith MZ, et al. Cerebrovascular disease and threshold for dementia in the early stages of Alzheimer's disease. Lancet 1999;354:919–20
53. Simons M, Schwarzler F, Lutjohann D, et al. Treatment with simvastatin in normocholesterolemic patients with Alzheimer's disease: A 26-week randomized, placebo-controlled, double-blind trial. Ann Neurol 2002;52:346–50
54. Fassbender K, Simons M, Bergmann C, et al. Simvastatin strongly reduces levels of Alzheimer's disease beta-amyloid peptides Abeta 42 and Abeta 40 in vitro and in vivo. Proc Natl Acad Sci U S A 2001;98:5856–61

Received April 25, 2003
Revision received September 8, 2003
Accepted September 11, 2003